Size dependence of self-diffusion in a dense hard-disc liquid

2000 J. Phys.: Condens. Matter 12 6563

(http://iopscience.iop.org/0953-8984/12/29/328)

J. Phys.: Condens. Matter **12** (2000) 6563–6573. Printed in the UK PII: S0953-8984(00)11495-X

Size dependence of self-diffusion in a dense hard-disc liquid

K Froböse, F Kolbe and J Jäckle†

Faculty of Physics, University of Konstanz, Konstanz, Germany

Received 1 February 2000

Abstract. For a binary liquid mixture of hard discs well above the freezing density of the one-component liquid the size dependence of the self-diffusion coefficients of small and large particles is calculated by molecular dynamics simulation. The observed size effect can be satisfactorily explained by the size-dependent cut-off of long-wavelength fluctuations of transverse collective flow and gives no indication of the importance of more 'cooperative' processes at high densities.

1. Introduction

In dense liquids composed of molecules with weak attractive forces the diffusive molecular motions are controlled by steric hindrance arising from the strong repulsive forces. The constraint becomes most severe for supercooled liquids approaching their glass transition. Due to the steric hindrance the diffusive displacements of the molecules must be highly coordinated. We address the question of how this coordination is organized geometrically and how the geometric pattern of coordinated particle displacements can be characterized. In systems of finite size, the presence of (rigid or periodic) boundaries strongly affects the coordination of particle motion, particularly if this occurs on a large length scale. Therefore, probing self-diffusion in systems of finite size [1–3] may help to answer these questions.

In general, we can distinguish displacement patterns according to their characteristic wavelength. Patterns of long wavelengths compared to the mean inter-particle distance and of short wavelengths comparable to that distance are extreme and opposite cases. In the first case displacement vectors vary but little from particle to particle, resulting in a pattern of coherent flow. In the second case neighbouring particles may be displaced in different directions. In this second case the displacement pattern may still correspond to coherent particle motions, as in an assembly of small vortex rings [4], but may also be more chaotic.

Which of these different possibilities prevails for a particular liquid or liquid model should depend on the shape of the liquid molecules and their density. For molecules of complicated non-spherical shape, which may interlock at high packing density [5], schematic lattice-gas models with kinetically constrained single-particle hopping were proposed [6–8]. For these models, the pattern of coordinated particle hops is irregular and resembles a sliding-piece puzzle game. The coordination of particle hopping has been described in anthropomorphic terms as a superposition of 'cooperative processes' [9, 10]. In systems of finite size, the cutting off of these processes leads to a marked size-dependent reduction of the self-diffusion coefficient.

† Author to whom any correspondence should be addressed.

0953-8984/00/296563+11$30.00

These lattice-gas models lack the possibility of collective flow of particles, which is the simplest mode of particle motion by which overlap can be avoided. The fingerprint of collective particle flow was detected long ago in the molecular dynamics (MD) of a 2d hard-disc liquid [11, 12] in equilibrium. It was found that the mean velocity field which develops around a reference particle with given initial velocity corresponds to a double vortex as described in hydrodynamics. More recently, evidence for collective particle flow has also been found in MD simulations of binary soft-disc liquids in the supercooled state at higher density [13–15]. The early observation [12] of a long-time tail $\propto t^{-1}$ of the velocity-autocorrelation function (VAF) $\langle \vec{v}(t) \cdot \vec{v}(0) \rangle$ could be explained by the fact that the reference particle itself is carried along by the mean velocity field that it generated [12, 16]. For finite systems, the cutting off of long-wavelength modes of hydrodynamic flow [17] leads to a logarithmic size dependence of D_s. In the present paper this theory of the size dependence of D_s is extended to high densities where the hydrodynamics needs to be generalized, and quantitatively tested using MD simulation. The question to be answered by this investigation is that of whether even at higher densities near random close packing the size dependence of D_s is governed by the size dependence of the modes of collective flow. A positive answer to this question will support the view that collective flow is always a prevalent feature in patterns of diffusive particle motions in this two-dimensional liquid, whereas a negative answer might point to the growing influence at higher densities of a more complicated type of particle coordination.

Our model is described in section 2. In section 3 a transverse and a longitudinal displacement structure factor are introduced for the statistical characterization of displacement patterns. The MD results for the size dependence of D_s are presented in section 4. In section 5 the theory relating the size-dependent part of D_s to the transverse and longitudinal current–current correlation functions is outlined. Results and conclusions are presented in section 6.

2. The model

The model liquid is an equimolar mixture of hard discs with a size ratio $\alpha = R_</R_> $ of 0.77. For this size ratio the binary liquid neither crystallizes nor demixes if compressed beyond the maximum concentration $c_f = 0.761$ of the one-component liquid [18]. This observation is compatible with the phase diagrams calculated by Speedy [19] for equimolar binary mixtures of hard discs with various size ratios, which develop a deep eutectic. Similar behaviour was reported for binary mixtures of soft discs by Bocquet *et al* [20], Perera and Harrowell [21], and also by Yamamoto and Onuki [22]. The concentration c is defined as the fraction of occupied area ϕ relative to hexagonal close packing:

$$c = \phi/\phi_{\text{h.c.p.}} \qquad \phi_{\text{h.c.p.}} = \pi/\sqrt{12}.$$

For the present study we chose a high concentration of $c = 0.85$. We performed MD simulations for N from 64 to 4096 particles with periodic boundary conditions in a rectangular box ($L_y/L_x = \sqrt{3}/2$). The unit of length is the radius $R_<$ of the smaller species of particles. The unit of time is chosen to make the mean square velocity equal to unity:

$$\langle \vec{v}^2 \rangle = \langle v_x^2 \rangle + \langle v_y^2 \rangle = 1.$$

3. Displacement patterns and displacement structure factors

The displacement pattern of figure 1 gives direct evidence of the importance of collective flow in particle diffusion. The figure shows a snapshot of the configuration of particles in a small part of a 4096-particle system. The dashes represent the displacements which occurred

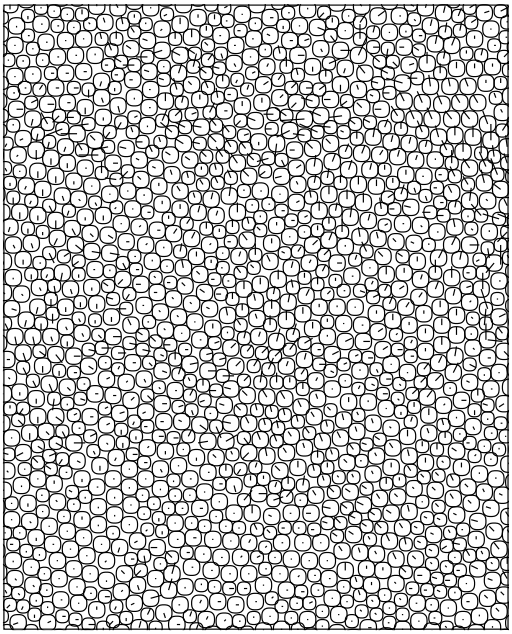

Figure 1. An example of a displacement pattern.

during the preceding time interval of length $\Delta t = 50$, which corresponds to an average number of 670 collisions per particle. Many particles occur in patches of nearly coherent flow, where the displacement vectors vary only little from particle to particle. In such regions some continuous lines of relatively large displacements can be found. Usually several such lines occur in parallel; occasionally it is only a single line. Sometimes such lines form (imperfect) closed loops. Besides these patterns of long-wavelength collective flow, there are regions in which the displacement pattern is more irregular. Looking more closely, here one can often find small vortex rings. 'Bond breaking' [23] of pairs of nearest-neighbour particles occurs primarily in such regions.

The visual observation of collective flow may be quantified in different ways. In their study of a supercooled binary liquid of soft discs Muranaka and Hiwatari [13, 14] introduced 'correlated motion coefficients' to measure the degree of coherent flow in a shell of neighbours around particles. Here we propose a longitudinal and a transverse 'displacement structure factor' $S^{(l,t)}_{w,w}(\vec{k};\Delta t)$ as a means of characterizing displacement patterns. They are defined as

$$S^{(l)}_{w,w}(\vec{k};\Delta t) = \left\langle \left| \frac{1}{\sqrt{N}} \sum_{l=1}^{N} \exp[\mathrm{i}kx_l(\Delta t/2)]\big(x_l(\Delta t) - x_l(0)\big) \right|^2 \right\rangle \tag{3.1a}$$

$$S^{(t)}_{w,w}(\vec{k};\Delta t) = \left\langle \left| \frac{1}{\sqrt{N}} \sum_{l=1}^{N} \exp[\mathrm{i}kx_l(\Delta t/2)]\big(y_l(\Delta t) - y_l(0)\big) \right|^2 \right\rangle \tag{3.1b}$$

$(\vec{k} = k\vec{e}_x)$.

$x_l(\Delta t/2)$ is the x-coordinate of particle l in the middle of the time interval during which the displacement $\vec{r}_l(\Delta t) - \vec{r}_l(0)$ is recorded. If k and Δt are small enough that $\exp[\mathrm{i}kx_l(t')]$ is practically constant in the time interval $0 < t' < \Delta t$, these displacement structure factors can be expressed as double-time integrals over the longitudinal and transverse current–current

correlation function $S^{(l,t)}_{j,j}(\vec{k},t)$:

$$S^{(\alpha)}_{w,w}(\vec{k};\Delta t) \sim \int_0^{\Delta t} \mathrm{d}t' \int_0^{\Delta t} \mathrm{d}t''\, S^{(\alpha)}_{j,j}(\vec{k},t'-t'') \qquad (\alpha = l,t). \tag{3.2}$$

For general wavevector $\vec{k}$, the two current–current correlation functions are defined as

$$S^{(l)}_{j,j}(\vec{k},t) = \langle j_l(\vec{k},t)(j_l(\vec{k},0))^*\rangle \tag{3.3a}$$

$$S^{(t)}_{j,j}(\vec{k},t) = \langle \vec{j}(\vec{k},t)\cdot(\vec{j}(\vec{k},0))^*\rangle - S^{(l)}_{j,j}(\vec{k},t) \tag{3.3b}$$

with

$$j_l(\vec{k},t) = \hat{k}\cdot\vec{j}(\vec{k},t) \qquad \hat{k} = \vec{k}/k \tag{3.4}$$

and

$$\vec{j}(\vec{k},t) = \frac{1}{\sqrt{N}}\sum_{l=1}^{N} \exp[\mathrm{i}\vec{k}\cdot\vec{r}_l(t)]\vec{v}_l(t). \tag{3.5}$$

In figure 2 $S^{(t)}_{w,w}(k;\Delta t)$ is plotted against k for the smallest k-values which fit into the 4096-particle system with $\Delta t = 8$, 16, and 32. At $\Delta t = 32$ the mean square displacement of the smaller particles is 1. The dotted lines were obtained by fitting $a_{\Delta t}/k^2$ to the data in the range from $2\,k_{\min}$ to $k = 0.2$. The data for $\Delta t = 32$ are well fitted by the k^{-2}-law, whereas the data at $k_{\min}$ for $\Delta t = 8$ and 16 are distinctly smaller than $a_{\Delta t}/k^2_{\min}$, which indicates that this law is not valid for $\Delta t \to 0$. With $S^{(t)}_{j,j}(k;t=0) = 1/2$, for small t we obtain from (3.2) for small Δt and small k

$$S^{(t)}_{w,w}(k;\Delta t) \sim \frac{1}{2}\,\Delta t^2 \tag{3.6}$$

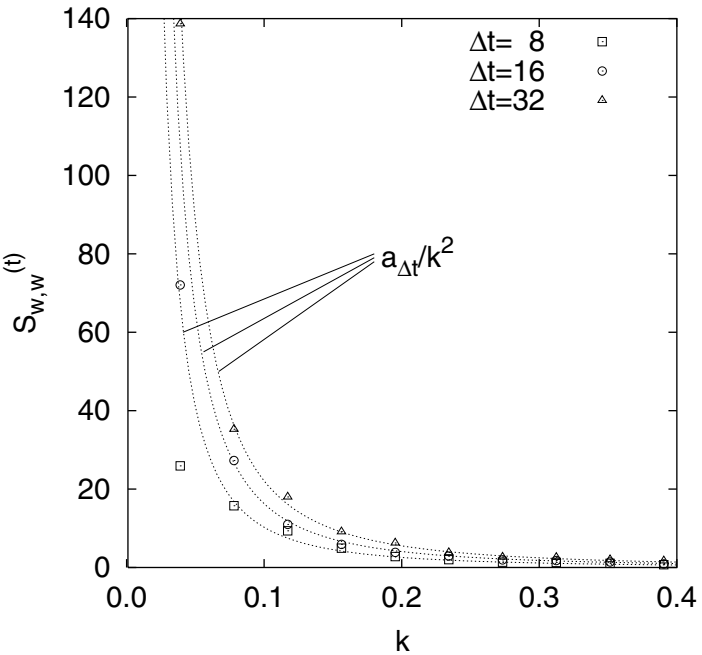

Figure 2. The wavevector dependence of the structure factor of transverse displacements. Dotted lines: fits to $a_{\Delta t}/k^2$ with $a_8 = 0.103$, $a_{16} = 0.163$, and $a_{32} = 0.221$ for time intervals of length Δt.

which yields 32 for $\Delta t = 8$. This is close to our MD result $S^{(t)}_{w,w}(k_{\min};\, \Delta t = 8) = 26$.

The longitudinal displacement structure factors $S^{(l)}_{w,w}(k;\, \Delta t)$ show similar behaviour, but are much smaller. In this sense, displacement patterns like the one shown in figure 1 are dominated by the contribution of transverse current fluctuations of the longest possible wavelengths. This result fits together with the explanation in reference [12] of the long-time tail of the VAF by a vortex-like correlation of the motion of neighbouring particles relative to the motion of a central particle.

An independent length of dynamic heterogeneity, as has been derived from the spatial distribution of 'broken bonds' [22, 23], is not apparent from these results.

4. Size dependence of the self-diffusion coefficient (D_s)

As is well known, the self-diffusion coefficient of a 2d liquid is infinite, because in 2d the long-time tail of the velocity-autocorrelation function is not integrable [12, 16]. For finite systems with periodic boundary conditions, however, this long-time tail becomes integrable, yielding a finite value of D_s. To obtain this finite value by MD, one needs to derive the mean square displacement from continuous trajectories in the periodically continued infinite system [17].

Figure 3 shows the size dependence of the self-diffusion coefficient $D_s^<$ of the smaller particles at concentration $c = 0.85$, together with three other concentrations. The size dependence is approximately logarithmic and amounts to more than a factor of 2 between the smallest and the largest systems with 64 and 4096 particles. A logarithmic size dependence of the self-diffusion coefficient is explained by the hydrodynamic theory of the long-time tail of the VAF [17]. It derives from the exponential form $\propto \exp(-\nu k^2 t)$ of the transverse current–current correlation function $S^{(t)}_{j,j}(k, t)$ (ν is the kinematic viscosity). However, at high concentrations

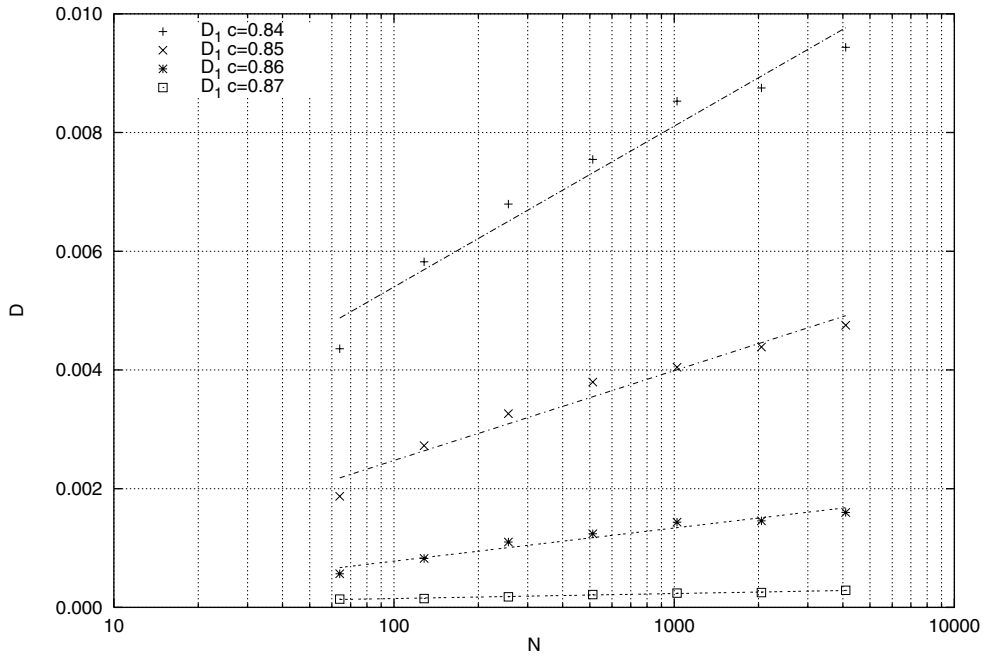

Figure 3. The dependence of the self-diffusion coefficient $D_s^<$ of the smaller discs on the particle number N at fixed concentration ($c = 0.85$).

like $c = 0.85$, we find a damped oscillatory behaviour of $S^{(t)}_{j,j}(k,t)$ rather than a monotonic decay. Therefore the hydrodynamic theory of the long-time tail of the VAF needs to be generalized by taking viscoelastic behaviour into account.

5. Calculation of the size dependence of D_s from current–current correlation functions

To establish a relation between the self-diffusion coefficient D_s and the longitudinal and transverse current–current correlation function $S^{(l)}_{j,j}(\vec{k},t)$ and $S^{(t)}_{j,j}(\vec{k},t)$ we argue as follows.

D_s is given by the time integral of the VAF:

$$D_s = \frac{1}{2}\int_0^\infty \langle \vec{v}(0)\cdot\vec{v}(t)\rangle \,\mathrm{d}t \qquad \text{in 2d.} \tag{5.1}$$

We express the VAF by the conditional VAF $\langle \vec{v}(0)\cdot\vec{v}(t)\rangle_{\vec{r}}$ derived from the subset of particles which are displaced by $\vec{r}$ during the time t:

$$\langle \vec{v}(0)\cdot\vec{v}(t)\rangle = \int \mathrm{d}^3 r \; p_t(\vec{r}|0)\langle \vec{v}(0)\cdot\vec{v}(t)\rangle_{\vec{r}}. \tag{5.2}$$

Here the long-time form of the displacement probability density

$$p_t(\vec{r}|0) = (4\pi D_s t)^{-1}\exp\left(-\frac{r^2}{4D_s t}\right) \tag{5.3}$$

is used. We now assume that the conditional VAC at long times is equal to the velocity–velocity correlation function of collective current fluctuations in the liquid, namely

$$\langle \vec{v}(0)\cdot\vec{v}(t)\rangle_{\vec{r}} = \langle \vec{v}(\vec{0},0)\cdot\vec{v}(\vec{r},t)\rangle = \frac{1}{n_0^2}\langle \vec{j}(\vec{0},0)\cdot\vec{j}(\vec{r},t)\rangle. \tag{5.4}$$

The last expression in (5.4) follows in a linear approximation, where $n_0 = N/\Omega$ is the mean particle density. Taking spatial Fourier transforms, the VAF at long times can be written as

$$\langle \vec{v}(0)\cdot\vec{v}(t)\rangle = \frac{1}{N}\sum_{\vec{k}\neq 0}\exp(-D_s k^2 t)\left\{S^{(l)}_{j,j}(\vec{k},t) + S^{(t)}_{j,j}(\vec{k},t)\right\} \tag{5.5}$$

where wavevectors

$$\vec{k} = 2\pi\left((n_x/L_x)\vec{e}_x + (n_y/L_y)\vec{e}_y\right) \tag{5.6}$$

are summed over all integers n_x and n_y (except $\vec{k} = 0$). The $\vec{k}$-vectors in the first quadrant for which the $\vec{k}$-summation in expression (5.5) is evaluated are shown in figure 4. Large dots are $\vec{k}$-vectors for both large ($N = 4096$) and small ($N = 64$) systems; small dots are $\vec{k}$-vectors only for the large system. For the large system $k_{x,\min} = 0.039$ (for unit length given by the radius $R_<$ of the small discs). To ensure that the number of $\vec{k}$-values (including zero) is proportional to N for both sizes, for the large system the $\vec{k}$-vectors with the largest k_x and/or k_y ($k_{x,\max} = 20\,k_{x,\min}$, $k_{y,\max} = 20\,k_{y,\min}$) are given a weight 1/2 at edge points and 1/4 at corner points. To separate out the long-time tail of the VAF, to which components with large wavevector do not contribute, we finally add a Gaussian cut-off factor $\exp(-(k/k_c)^2)$ on the r.h.s. of equation (5.5).

The longitudinal and transverse current–current correlation functions $S^{(l)}_{j,j}(\vec{k},t)$ and $S^{(t)}_{j,j}(\vec{k},t)$, which are defined in (3.3)–(3.5), are calculated numerically by means of MD in a standard way. To obtain good data, we had to take time averages in addition to averages over different samples. In order to perform the time integration, we fit them to analytical expressions which can be derived from viscoelastic theory and which read

$$S^{(l)}_{j,j}(\vec{k},t) = \mathrm{e}^{-\Gamma_l(\vec{k})t}\left\{A_l(\vec{k})\cos\left(\Omega_l(\vec{k})t\right) + B_l(\vec{k})\sin\left(\Omega_l(\vec{k})t\right)\right\} + C_l(\vec{k})\mathrm{e}^{-\kappa(\vec{k})t} \tag{5.7}$$

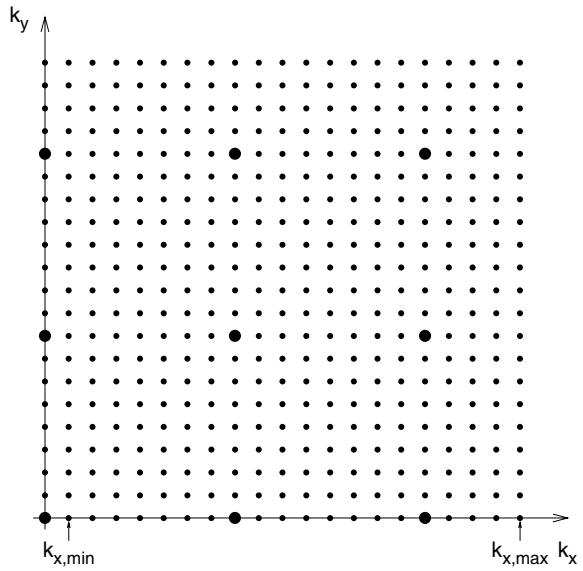

Figure 4. The wavevectors in the first quadrant taken into account in the sum of expression (5.16). See the text.

and

$$S^{(t)}_{j,j}(\vec{k},t) = \mathrm{e}^{-\Gamma_t(\vec{k})t}\left\{A_t(\vec{k})\cos\bigl(\Omega_t(\vec{k})t\bigr) + B_t(\vec{k})\sin\bigl(\Omega_t(\vec{k})t\bigr)\right\}. \tag{5.8}$$

All parameters occurring in these expressions are treated as free $\vec{k}$-dependent fit parameters. The functional form of expression (5.7) for the longitudinal correlation function, which consists of a damped oscillatory and an exponentially relaxing term, is familiar both from hydrodynamics and from the theory of viscoelasticity. The damped oscillatory behaviour of expression (5.8) for the transverse case, however, is characteristic of viscoelasticity, and differs from the hydrodynamic form of exponential decay noted above.

The MD data are fitted by the expressions (5.7) and (5.8) within numerical accuracy. The occasionally observed differences between the fit and the MD data are so small that there is no necessity to apply more complicated functional forms.

We now briefly show how the form of expression (5.7) and (5.8) can be derived from equations of motion with a memory integral containing a single exponential as its memory kernel. Let us consider the transverse case first. Here the equation of motion reads

$$\left(\frac{\partial}{\partial t} + \beta_t(\vec{k})\right)S^{(t)}_{j,j}(\vec{k},t) + \omega^2_\infty(\vec{k})\int_0^t \mathrm{d}t' \exp[-\gamma_t(\vec{k})(t-t')]S^{(t)}_{j,j}(\vec{k},t') = 0 \tag{5.9}$$

from which the initial condition

$$\dot{S}^{(t)}_{j,j}(\vec{k},t=0) = -\beta_t(\vec{k})S^{(t)}_{j,j}(\vec{k},t=0) \tag{5.10}$$

follows. In the longitudinal case, the current–current correlation function is related, via the continuity equation, to the density–density correlation function $S_{n,n}(\vec{k},t)$ by

$$S^{(l)}_{j,j}(\vec{k},t) = -\frac{\partial^2}{\partial t^2}S_{n,n}(\vec{k},t)/k^2 \tag{5.11}$$

where the latter function obeys the equation of motion

$$\left(\frac{\partial^2}{\partial t^2} + \beta_l(\vec{k})\,\frac{\partial}{\partial t} + \omega_0^2(\vec{k})\right) S_{n,n}(\vec{k},t) + \Delta^2(k)\int_0^t \exp[-\gamma_l(\vec{k})(t-t')]\dot{S}_{n,n}(\vec{k},t')\,\mathrm{d}t' = 0 \tag{5.12}$$

with the initial condition

$$\dot{S}_{n,n}(\vec{k}, t=0) = 0. \tag{5.13}$$

From (5.11) and (5.12) the initial conditions for the current-correlation function

$$\dot{S}^{(l)}_{j,j}(\vec{k}, t=0) = -\beta_l S^{(l)}_{j,j}(\vec{k}, t=0) \tag{5.14}$$

$$\ddot{S}^{(l)}_{j,j}(\vec{k}, t=0) = -(\omega_0^2 + \Delta^2 - \beta_l^2) S^{(l)}_{j,j}(\vec{k}, t=0) \tag{5.15}$$

are derived. With initial conditions (5.10) and (5.14), (5.15), respectively, the solutions $S^{(t)}_{j,j}(\vec{k},t)$ and $S^{(l)}_{j,j}(\vec{k},t)$ of equations (5.9) and (5.11)–(5.13) contain four and five free parameters, respectively, including the initial values $S^{(t)}_{j,j}(\vec{k},0)$ and $S^{(l)}_{j,j}(\vec{k},0)$. Because of the inaccuracy of our numerical data it is appropriate to compare with solutions for which these initial values are not fixed. In the transverse case this is the same number as the number of free parameters used in fitting expression (5.8). Therefore the fit (5.8) of the transverse current–current correlation function is always a solution of an equation of type (5.9). In the longitudinal case, on the other hand, the number of fit parameters in expression (5.7) exceeds the number of parameters in the solution of equations (5.11)–(5.13) by one. Therefore the fit (5.7) of a longitudinal function does not necessarily satisfy both initial conditions (5.14), (5.15). Using the first of these conditions to determine the parameters β_l, ω_0^2, Δ^2, and γ_l we find that the second one is fulfilled to better than 10% only for small wavevectors $k < 6\,k_{x,\min}$. We verified that both for the transverse and the longitudinal case the fits (5.7), (5.8) always correspond to positive values of the parameters occurring in the equations of motion (5.9), (5.12), as they should.

Combining equations (5.1), (5.5), (5.7), and (5.8) with a Gaussian cut-off factor included in (5.5), as was already mentioned, we obtain the contribution of long-wavelength fluctuations of collective flow to the self-diffusion coefficient as

$$D_s(N)\big|_{\text{Coll. flow}} = \frac{1}{2N}\sum_{\vec{k}\neq 0}\exp[-(k/k_c)^2]\left\{\frac{A_t(\vec{k})\big[D_s k^2 + \Gamma_t(\vec{k})\big] + B_t(\vec{k})\Omega_t(\vec{k})}{\big[D_s k^2 + \Gamma_t(\vec{k})\big]^2 + \big(\Omega_t(\vec{k})\big)^2}\right.$$
$$\left. + \frac{A_l(\vec{k})\big[D_s k^2 + \Gamma_l(\vec{k})\big] + B_l(\vec{k})\Omega_l(\vec{k})}{\big[D_s k^2 + \Gamma_l(\vec{k})\big]^2 + \big(\Omega_l(\vec{k})\big)^2} + \frac{C_l(\vec{k})}{D_s k^2 + \kappa(\vec{k})}\right\}. \tag{5.16}$$

We found that the additive term $D_s k^2$ is always negligible compared with $\Gamma_l(\vec{k})$, $\Gamma_t(\vec{k})$, and $\kappa(\vec{k})$. We evaluated the difference of this expression between $N = 4096$ and $N = 64$.

6. Results and conclusions

In figure 5(a) the longitudinal and transverse current–current correlation functions for the smallest wavevector $\vec{k}_{\min} = k_{x,\min}\vec{e}_x$ of the large system are shown together with their fit to expressions (5.7) and (5.8). Figure 5(b) shows the same for the largest wavevector $\vec{k}_{\max} = 20\,\vec{k}_{\min}$ which we took into account for the large system. The MD data were obtained in the following way: before averaging over different samples, time-averaged correlation functions were calculated from $\vec{j}(\vec{k},t)$ data taken over a time interval of length $\Delta t = 500$. We note that in the fits of the longitudinal functions to expression (5.7) the coefficients $C_l(\vec{k})$

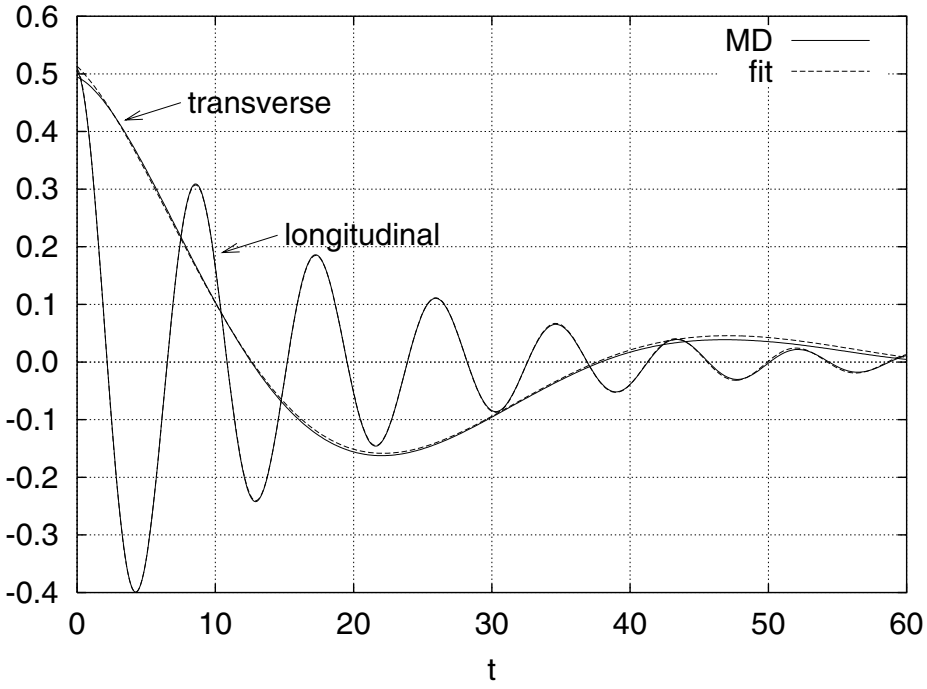

(a)

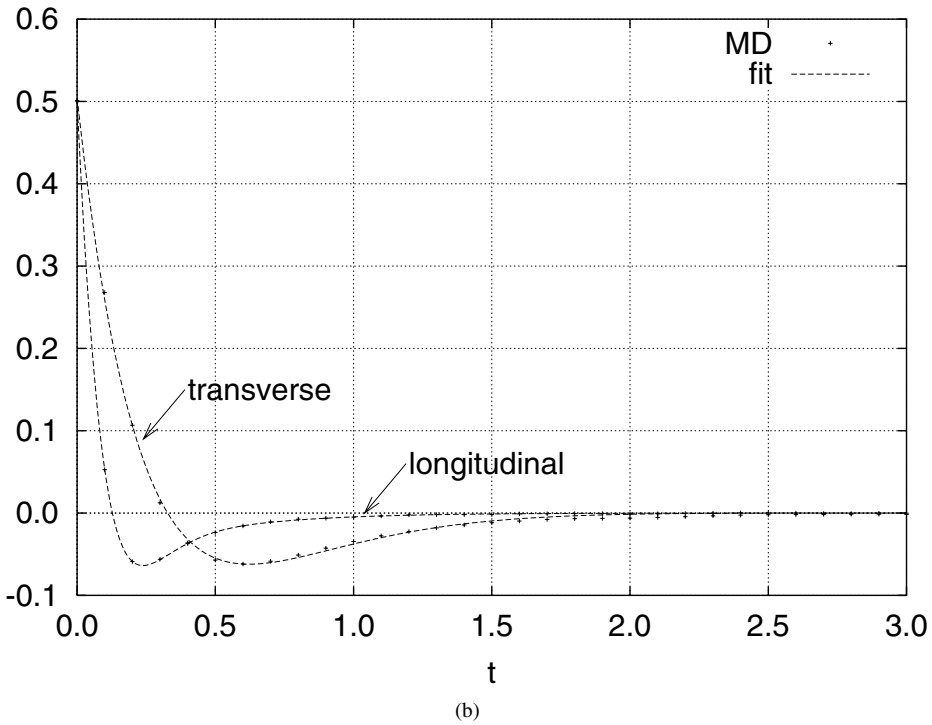

(b)

Figure 5. Time dependences of the longitudinal and transverse current–current correlation functions at the smallest (a) and largest (b) wavevector in the x-direction for the large system ($N = 4096$).

of the exponential term $\propto \exp(-\kappa(\vec{k})t)$ are always negative. This is a consequence of relation (5.11) in which the coefficient of the exponential term is reversed. As a consequence, the Fourier transform $S^{(l)}_{j,j}(\vec{k}, \omega)$ contains no quasi-elastic contribution (centred at $\omega = 0$), unlike the Fourier transform $S_{n,n}(\vec{k}, \omega)$.

In figure 6 the MD data for the longitudinal and the transverse correlation functions for the large and the small systems are compared for the $\vec{k}$-vector $\vec{k} = 8\,\vec{k}_{\min}$, which is common to both system sizes. The difference is surprisingly small. Obviously the viscoelastic coefficients determining these functions depend only weakly on system size.

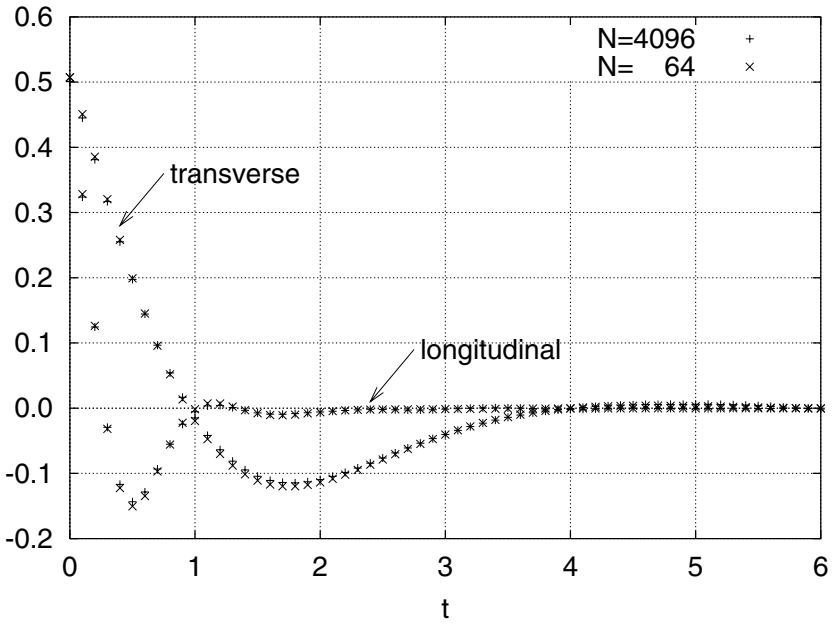

Figure 6. Comparison of the longitudinal and transverse current–current correlation functions at intermediate wavevector for small ($N = 64$) and large ($N = 4096$) systems.

Using these results for the longitudinal and transverse current–current correlation functions, expression (5.16) can be evaluated for the large ($N = 4096$) and the small ($N = 64$) system. It depends on the choice of k_c in the cut-off factor. For k_c between $8\,k_{x,\min} = 0.312$ and infinity (i.e. no cut-off factor), the difference of the two self-diffusion coefficients varies between 2.42×10^{-3} and 3.08×10^{-3}. We therefore estimate

$$D_s(N = 4096) - D_s(N = 64)\big|_{\text{Coll. flow}} = 2.5 \times 10^{-3} \tag{6.1}$$

with an uncertainty of about 20%. We found that the contribution of the longitudinal fluctuations amounts only to 2% of this result†.

We compare the contribution (6.1) of collective flow to the size dependence of the D_s-data obtained directly from MD. The difference in the self-diffusion coefficient $D_s^<$ of the small particles between the large and the small system is

$$D_s^<(N = 4096) - D_s^<(N = 64) = 2.90 \times 10^{-3}. \tag{6.2}$$

† The result for this contribution is actually due to numerical inaccuracies. Once it is recognized that in expression (5.5) the diffusion factor $\exp(-D_s k^2 t)$ can be neglected, the longitudinal contribution without this factor should be strictly zero, since it follows from (5.11) and (5.13) that the time integral over $S^{(l)}_{j,j}(\vec{k}, t)$ is zero.

For the large particles the same difference amounts to

$$D_s^{>}(N = 4096) - D_s^{>}(N = 64) = 2.33 \times 10^{-3}. \tag{6.3}$$

In the above calculation of the VAF from current–current correlation functions we did not distinguish between large and small particles. It is therefore plausible to compare the result (6.1) with the arithmetic mean $\overline{D}_s$ of the self-diffusion coefficients for the large and the small particles. The difference between the values of $\overline{D}_s$ for the two sizes is

$$\overline{D}_s(N = 4096) - \overline{D}_s(N = 64) = 2.61 \times 10^{-3}. \tag{6.4}$$

This is within the margin of uncertainty of the calculated result (6.1).

From this good agreement between (6.1) and (6.4) we conclude that the size dependence of the self-diffusion coefficients in the binary hard-disc liquid of high concentration $c = 0.85$ arises mainly from the fluctuations of transverse collective flow of long wavelength, as in the case of lower densities. The size effect on self-diffusion therefore gives no indication of the importance at high density of more 'cooperative' processes, by means of which steric hindrance would be avoided in a more complicated way.

References

[1] Fehr T and Löwen H 1995 *Phys. Rev.* E **52** 4016
[2] Németh Z T and Löwen H 1999 *Phys. Rev.* E **59** 6824
[3] Kim K and Yamamoto R 1999 *Preprint* cond-mat/9903260
[4] Feynman R P 1954 *Phys. Rev.* **94** 262
[5] Ubbelohde A R 1978 *The Molten State of Matter* (Chichester: Wiley) section 13.6
[6] Ertel W, Froböse K and Jäckle J 1988 *J. Chem. Phys.* **88** 5027
[7] Jäckle J and Krönig A 1994 *J. Phys.: Condens. Matter* **6** 7633
[8] Jäckle J 1997 *Prog. Theor. Phys. Suppl.* **126** 53
[9] Jäckle J 1994 *Disorder Effects on Relaxational Processes* ed R Richert and A Blumen (Berlin: Springer) p 233
[10] Jäckle J 1996 *Non-Equilibrium Phenomena in Supercooled Fluids, Glasses and Amorphous Materials* ed M Giordano, D Leporini and M P Tosi (Singapore, World Scientific) p 41
[11] Alder B J and Wainwright T E 1969 *J. Phys. Soc. Japan Suppl.* **26** 267
[12] Alder B J and Wainwright T E 1970 *Phys. Rev.* A **1** 18
[13] Muranaka T and Hiwatari Y 1995 *Phys. Rev.* **51** R2735
[14] Hiwatari Y and Muranaka T 1998 *J. Non-Cryst. Solids* **235–237** 19
[15] Perera D N and Harrowell P 1998 *J. Non-Cryst. Solids* **235–237** 314
[16] Ernst M H, Hauge E and van Leeuwen J M J 1971 *Phys. Rev.* A **4** 2055
[17] Erpenbeck J J and Wood W W 1982 *Phys. Rev.* A **26** 1648
[18] Hoover W G and Ree F H 1968 *J. Chem. Phys.* **49** 3609
[19] Speedy R J 1999 *J. Chem. Phys.* **110** 4559
[20] Bocquet L, Hansen J-P, Biben Th and Madden P 1992 *J. Phys.: Condens. Matter* **4** 2375
[21] Perera D N and Harrowell P 1999 *Phys. Rev.* E **59** 5721
[22] Yamamoto R and Onuki A 1997 *J. Phys. Soc. Japan* **66** 2545
[23] Yamamoto R and Onuki A 1998 *Phys. Rev.* E **58** 3515